18TH WORLD CONFERENCE ON EARTHQUAKE ENGINEERING
WCEE2024
MILAN

MILAN, ITALY
30TH JUNE - 5TH JULY 2024

www.wcee2024.it

SEISMIC DESIGN OF MODERN CLAY BRICK MASONRY STRUCTURES

S. Chatterji[1], N. Salentin[1], C. Butenweg[2], N. Boesen[3], & U. Meyer[4]

[1] Chair of Structural Analysis and Dynamics RWTH Aachen University, Aachen, Germany

[2] Center for Wind and Earthquake Engineering RWTH Aachen University, Aachen, Germany

[3] Basler & Hofmann AG Consulting Engineers, Zurich, Switzerland

[4] Bundesverband der Deutschen Ziegelindustrie e.V., Berlin, Germany

Abstract: *Modern masonry buildings made of brick masonry must not only meet the architectural requirements for transparency and user flexibility but also be optimally designed in terms of statics, energy, sound insulation, sustainability and fire protection. Due to complex interaction of the aforementioned requirements, structural verification of masonry buildings under horizontal actions, such as seismic actions, is often not possible at all or only at the limit with current simplified verification approaches. On the one hand, this is due to the fact that masonry has continuously developed with new innovative products and processes, while normative calculation models and design concepts still show significant potential for improvement despite intensive research activities in recent years. On the other hand, due to the target of climate neutrality by year 2045, a change is taking place from traditional solid construction to lightweight, resource-saving, and economical constructions, which also fundamentally change the boundary conditions for seismic design of masonry.*

The contribution presents the design of modern clay brick masonry structures based on a novel shear wall test database for clay brick masonry used in Germany with special attention to low vertical load levels and wall-slab interaction effects. Extensive cyclic shear wall results of the database are evaluated in terms of failure modes, load-bearing and deformation capacities and used as a basis for systematic numerical simulations. In addition, a nonlinear simulation model was developed in which the individual masonry units are represented by nonlinear material laws, whereas head and bed joints are idealized by contact elements. Systematic parametric studies with variations of vertical load level, moment distribution and wall slenderness ratio have been carried out with the model calibrated on small specimen tests. The three-dimensional simulation and test matrix was defined with the aim to cover occurring failure modes for boundary conditions in practice and to derive a new criterion for differentiation between bending and shear failure. Based on the extensive database, results for the load-bearing and deformation capacities as a function of the main influencing factors are presented. Finally, based on stress evaluations in shear walls, an outlook is given on the ongoing work to derive an improved shear design concept with a higher accuracy of prediction for seismically loaded masonry walls.

1. Database for German clay brick masonry

The basic idea of the database for clay brick masonry used in Germany is the structured data storage and evaluation of all relevant shear wall tests on modern clay brick masonry to create a comprehensive test grid that can be specifically complemented and condensed in the future. So far, the database contains shear walls made of different types of hollow clay bricks, executed with thin bed layer mortar. The following information are stored in the database for each shear wall: brick type and geometrical properties, material and strength properties of brick, mortar and masonry, boundary conditions, vertical load level, horizontal load history, hysteresis loops and their envelopes, energy dissipation for each hysteresis loop, bilinear approximation of the load-displacement curve and a detailed description of observed failure modes.

1.1. Composition of the database

The database includes in-plane cyclic shear wall tests executed in the European research initiative titled "Enhanced Safety and Efficient Construction of Masonry Structures in Europe" (ESECMaSE, 2007, 2008). This collaborative project was conducted among others at the University of Kassel (UNIK), the Technical University of Munich (TUM), and the University of Pavia (UniPV). Further cyclic shear wall tests were executed at the Slovenian National Building and Civil Engineering Institute (ZAG) in Ljubljana, at the University of Kassel (UNIK) and at the Center for Wind and Earthquake Engineering, RWTH Aachen University (CWE) on behalf of the Arbeitsgemeinschaft Mauerziegel e.V. (AGMz). Table 1 provides an overview of the conducted in-plane cyclic tests and basic information on the masonry units used for the shear walls tests. Detailed information about the boundary conditions and results of the shear wall tests can be found in the cited reports (Table 1).

Currently, the database consists of a total of 58 in-plane cyclic shear wall tests. A total of 48 tests were performed with the constant kinematic boundary condition “double fixed” which corresponds to a shear span of $h_0 = 0.5 \cdot h$. Only ten walls are tested with shear spans greater than 0.5 ranging up to $h_0 = 1.66 \cdot h$. The length of the walls varies between $1.0\ m$ and $2.265\ m$, whereas the height ranges from $2.5\ m$ and $2.75\ m$ which corresponds to typical storey heights. The investigated wall thicknesses are $175\ mm$ for interior walls and $300\ mm$, $365\ mm$ for exterior walls with higher thermal insulation properties. Figure 1 illustrates the distribution of specimens with respect to wall lengths and thicknesses. The ratio of the applied vertical stress and the characteristic compressive strength of masonry (σ_0/f_k) varies between $2.98\ \%$ and $46.75\ \%$. Figure 2 provides an overview of the number of tests performed within specific ranges of the σ_0/f_k ratio.

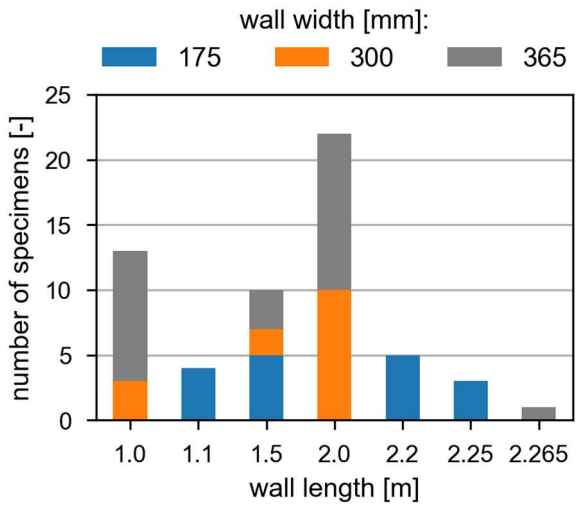

Figure 1: Number of tests for different wall lengths and wall thicknesses

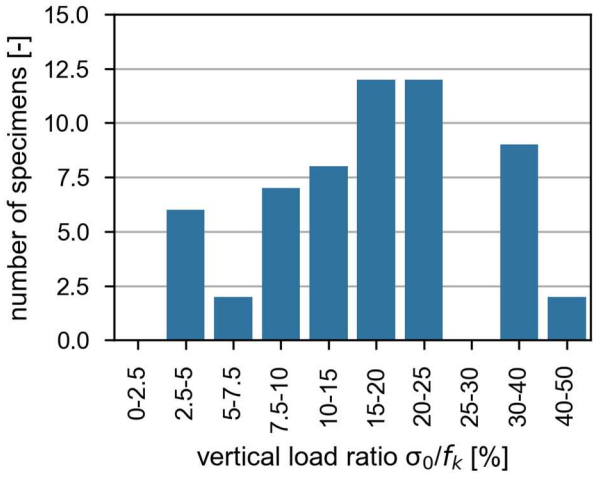

Figure 2: Number of tests for the given range of σ_0/f_k

Table 1: Overview: Test facility, number of shear wall tests and masonry units

Institution		No. of tests	Masonry unit(s)	
ESECMaSE	UNIK (ESECMaSE 2007)	1	HLZ-Plan-12-0.9	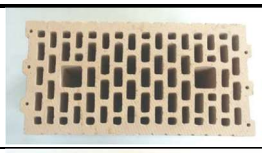
		3	HLZ-Plan-12-0.9 – optimized	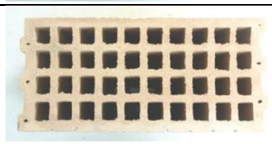
		5	HLZ-Plan-12-0.9 – optimized2	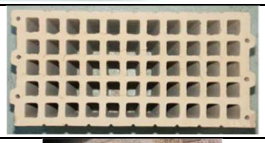
	TUM (ESECMaSE 2008)	1		
	UniPV (ESECMaSE 2008)	1	HLZ-Plan T16	
	UNIK (ESECMaSE 2007)	1	HLZ-Plan T10	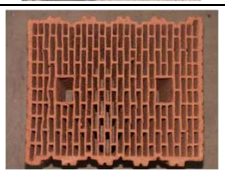
UNIK (Fehling, Stürz 2009)		1		
ZAG (ZAG 2018b)		10	UNIPOR WS10 CORISO	
ZAG (ZAG 2020d)		2		
ZAG (ZAG 2020a)		1		
ZAG (ZAG 2019)		6	Klimatherm PL9 1446	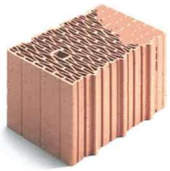
ZAG (ZAG 2020d)		1		
ZAG (ZAG 2018c)		6	ThermoPlan MZ70 HLZ B	
UNIK (Fehling, Pfetzing 2018)		2		
ZAG (ZAG 2017)		10	Thermopor TV9 - Plan	
CWE (Butenweg et. al. 2023)		7	POROTON Plan-T0.8	

The masonry walls of the tests were constructed with vertically perforated bricks using a thin-bed-layer mortar in the bed joints, while the head joints remained unfilled. The horizontal alignment of the walls was ensured by placing the first row of bricks on a layer of general-purpose mortar with a thickness up to 2 cm. For all types of bricks the compressive strength of brick and masonry, the initial shear strength of masonry under zero compressive stress and the shear strength were determined by standardized small specimen tests.

1.2. Test procedure

The comparability of the test results is guaranteed by uniform test conditions and a specific cyclic load application, which were proposed within the framework of ESECMaSE (2007, 2008) project (Schermer, 2008). This proposal forms also the basis for the definition of cyclic shear wall tests in the new generation of Eurocode 8 (prCEN/TS 1998-1-101, 2023). According to the test proposal, the cyclic tests on all unreinforced masonry walls within the database were conducted by imposing cyclic lateral drift demands to the specimen in either a sinusoidal or ramped manner, coupled with a constant axial load that was applied prior the lateral drift. The cyclic loading was usually always applied with three cycles at each drift angle up the maximum drift angle that can be estimated as the drift capacity at 20 % drop in horizontal strength. In most of the tests performed, smaller increments were applied at the beginning to capture the linear stiffness range more precisely. The drift increments were increased until the collapse of the wall was reached.

1.3. Failure modes

Generally, the failure modes of unreinforced masonry can be divided into flexural and shear failure modes. The formation of one of these specific failure modes depends on the wall geometry, the masonry and mortar strength, the ratio between horizontal and vertical loads and the moment distribution within the wall. Shear failures of unreinforced masonry walls subjected to in-plane seismic loading are typically characterized by diagonal cracks. If the compression stresses are quite low, shear failure takes place in the mortar joints while the bricks remain undamaged. For higher compression stresses, failures can also occur in the bricks as diagonal tension failures. This failure mode results from shear induced brick rotations which cause high tensile stresses in the bricks. Diagonal tension failure in the bricks is characterized by narrow hysteresis loops and moderate energy dissipation capacity. Slender masonry walls subjected to combined vertical and horizontal loading behave more like flexural beams with the formation of cracks due to bending stresses at the bottom of the wall. Subsequently, the failure modes are classified into shear failure (diagonal tension failure or sliding) and flexural failure. Since some walls cannot be clearly assigned to the dominant failure modes, a mixed failure mode is also introduced. Figure 3 shows the identified failure modes of the shear walls contained in the database. Most of the walls failed in shear, while a significantly smaller number of walls failed in flexure or with a mixed failure.

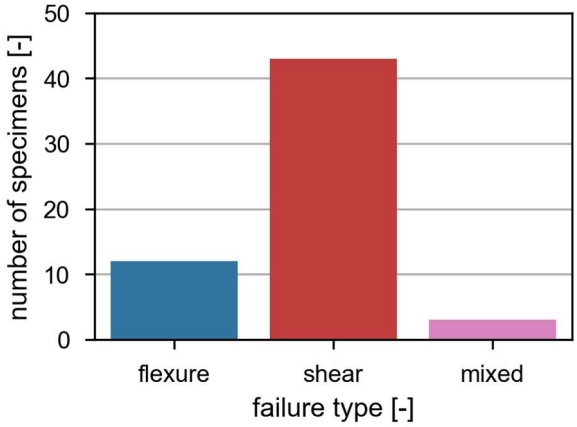

Figure 3: Number of tests with the identified failure modes

1.4. Envelopes of the load displacement curves

The analysis of the hysteresis loops recorded in the shear wall tests, performed automatically in the database, involves the generation of an envelope curve for the positive and negative loading directions. The obtained envelopes are the basis for the calculation of an idealized bilinear approximation to describe the load and deformation behavior of masonry shear walls (Frumento et al., 2009). Figure 4 shows the envelopes for both loading directions divided according to the failure modes encountered.

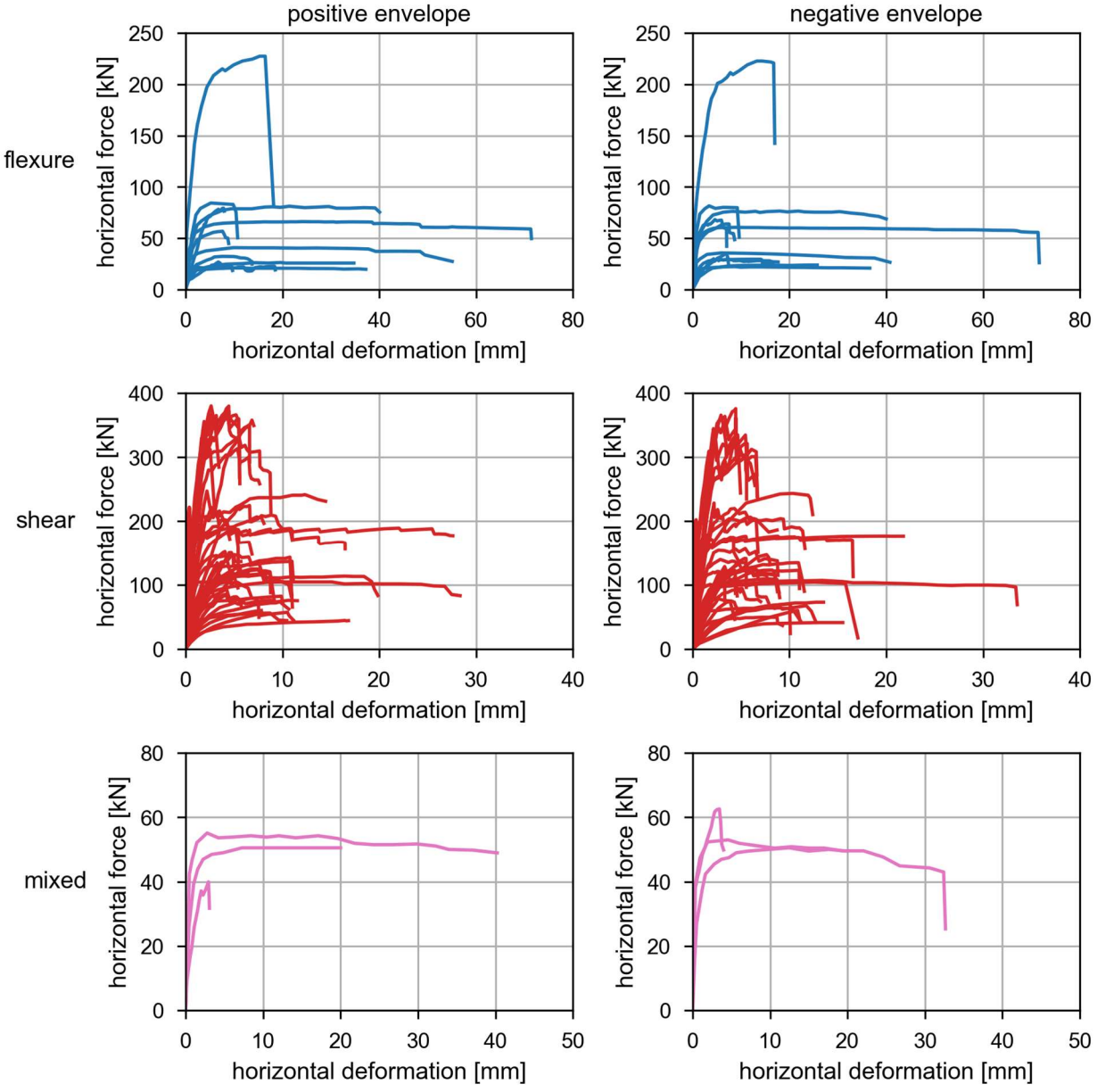

Figure 4: Negative (left) and positive (right) envelopes of all tests with respect to the failure mode

2. Numerical simulation

Due to the fact that experimental shear wall tests cause high costs and effort, only tests for a small selection of geometries, vertical loads and boundary conditions can be carried out. This underlines the need for numerical simulations to systematically investigate the failure modes and to fill the gaps of the experimental grid. Therefore, a nonlinear simulation model for masonry shear walls for combined vertical and horizontal in-plane loading is introduced in the following. The calibration of the model is carried out by means of small specimen test on bricks and masonry assemblies and validation is performed with the shear wall tests of the database. The model is further used for a systematic parametric study on masonry shear walls with variation

of the main influencing parameter. The results of the parametric are evaluated with respect to the maximum load, the deformation capacity, and the occurring failure modes. In this article, the application of the simulation model is presented as an example for the vertically perforated brick UNIPOR WS10 CORISO with the technical approval Z-17.1-1021 [Deutsches Institut für Bautechnik 2016].

2.1. Model description

The modelling of the masonry is based on a simplified micro model (Lourenco 1996; D'Altri et al. 2019, Schlegel 2004), in which an explicit idealization of the mortar joints is prevented by interface elements (Figure 5). This is justified, as the head joints are ungrouted and the bed joints are usually executed with thin-layer mortar with a thickness of about 1 mm. To consider transverse stresses within the wall plane arising from the interaction between brick and mortar, discrete finite element modeling in three dimensions is applied (Mistler 2006). The behaviour of the mortar and the contact between the bricks is assigned to interface elements between the masonry units. The bricks are modelled by homogenous solid elements discretized with volume elements. The perforation of the bricks is neglected. The behavior of the brick is described by the nonlinear Karagozian & Case concrete model (KCCM) (Malvar et al. 1997; Wu and Crawford 2015). To maintain realistic dimensions in the simplified micro-model, where the mortar joint has no geometric thickness, the bricks are extended by half of the bed joint thickness. The contact surfaces in the bed joints are represented by an interface element with a stress-based failure contact formulation and cohesive softening behavior. The DYCOSS Discrete Crack Model, as described in Lemmen et. al. (1999) and Schipperen (2012) is applied to accurately capture the adhesive properties between brick and mortar. The ungrouted butt joints are modeled as frictional contact with self-contact mechanism. For the numerical simulation, the Finite-Element Software LS-DYNA (LS-DYNA 2020) is used. Further details on the simulation model and are given in Boesen (2021).

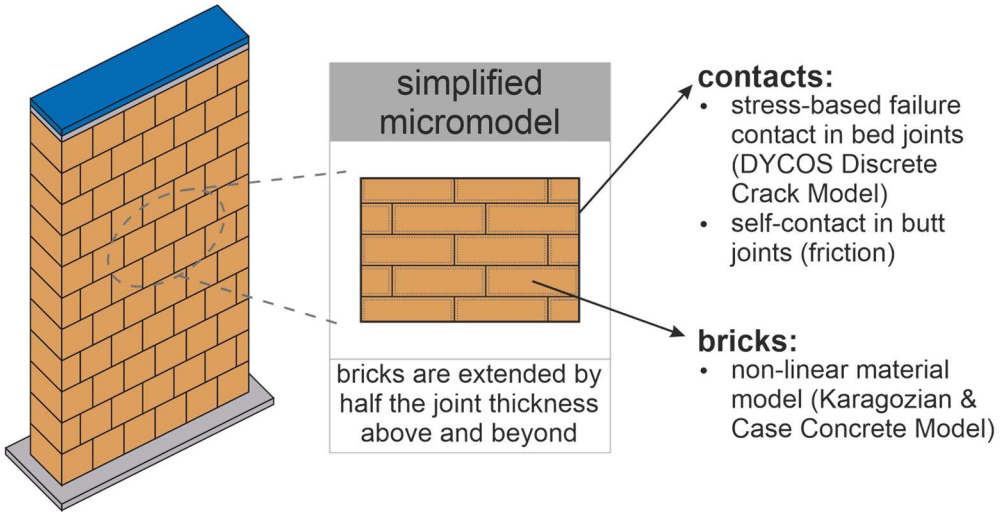

Figure 5: Shear wall and simplified micro-model (Boesen 2021)

2.2. Calibration

The calibration of the single components of the numerical model is systematically carried out by means of small specimen tests. At first, the material model for the brick is calibrated based on the uniaxial compression test, whereas the simulations on the brick are carried out deformation-controlled to reproduce the softening range. In the next step, the calibration of the DYCOSS model is performed with the already calibrated material model of the brick using the results of shear tests with three bricks according to Method A of DIN EN 1052-3 (2007). The numerical simulation model consists of three masonry units connected to each other via contact surfaces and thus accurately represents the shear test with three bricks. The material data taken into consideration are derived from investigations as per ZAG (2020a, 2020d, 2018b). A comprehensive summary of the calibrated strength and material parameters is presented in Table 2. The in Table 2 mentioned fracture energy corresponds to the energy required to form the fracture surface and can be calculated by the integral of the stress-displacement curve. Mode I describes bond behavior under tensile load while Mode II describes bond behavior under shear load.

Table 2: Calibrated parameters of the material and contact model (Boesen 2021)

Parameter	Value	Unit
Material model		
Cylindrical compressive strength $f_{cyl,m}$	7.296	$[N/mm^2]$
Stone tensile strength $f_{t,st}$	1.094	$[N/mm^2]$
Poisson's ratio ν	0.15	$[-]$
Contact model		
Adhesive tensile strength f_{n0}	0.10	$[N/mm^2]$
Adhesive shear strength f_{v0}	0.60	$[N/mm^2]$
Angle of internal friction μ	33.0	$[°]$
Fracture energy mode I -G_{Ic}	30.0	$[Nm/m^2]$
Fracture energy mode II - G_{IIc}	$350 \cdot \sigma + 67$	$[Nm/m^2]$

2.3. Validation

Following the calibration of the numerical models for the clay bricks and the bond behaviour of the joints the simulation model is validated with the results of 18 shear wall tests on the vertically perforated clay brick UNIPOR WS10 CORISO carried out at the laboratory ZAG (2020a, 2020d, 2018b). The detailed description of the experimental set-up and execution can be taken from the reports. Due to the complexity and calculation times, the application of the horizontal deformations is applied quasi-static. This represents an approximation, but still allows the analysis of the wall behavior and a sufficiently accurate estimation of the load-bearing and deformation capabilities of the wall. The validation of the simulation results is mainly based on the comparison of the simulated load-displacement curves with the enveloping curves of the cyclic tests in positive and negative loading direction. Furthermore, the stress and strain distribution as well as specific failure modes within the wall are analyzed and compared. Table 3 shows the comparison of the load-displacement curves and the principal strain distributions at maximum load and near collapse on the example of a short wall with $1.0\ m$ and a vertical load level of $\sigma_0/f_k = 16\ \%$. The ultimate Drift is determined right before the point where the load bearing capacity exceeds a $20\ \%$ degradation in comparison to the maximum load bearing capacity.

Table 3: Comparison of simulated and experimental results for a wall with a length of 1.0 m (Boesen 2021)

load-displacement-curves	principal strain distributions			
	experiment		numeric simulation	
	Max	*NC*	*Max*	*NC*
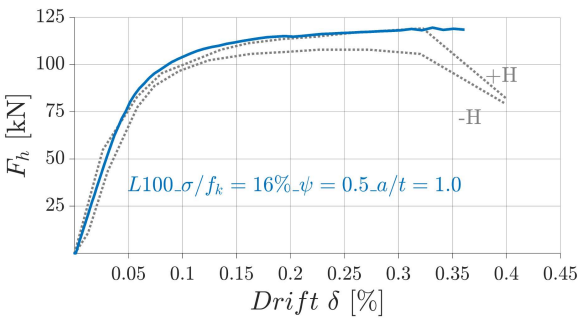		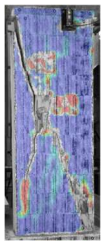	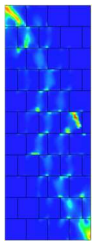	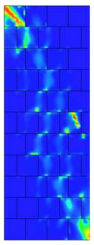

					exp	num	exp/num	failure mode
ψ	0.5	$[-]$						
a/t	1.0	$[-]$	$F_{H,max}$	$[kN]$	113	120	0.94	stone tensile failure
σ_0/f_k	16	[%]	δ_{ult}	[%]	0.40	0.36	1.11	

2.4. Parametric study

Utilizing the calibrated and validated numerical simulation model an extensive parametric study is carried out. The study considers the variation of all relevant influencing parameters affecting the load-bearing and deformation behavior of the shear walls:

- **Wall slenderness h/l**
  With a constant wall height of $h_w = 2.75\ m$, eight wall lengths of are simulated: $1.0\ m, 1.25\ m, 1.5\ m, 1.75\ m, 2.0\ m, 2.5\ m, 3.0\ m, 4.0\ m$. This corresponds to slenderness ratios between $h/l = 0.69$ and $h/l = 2.75$.
- **Axial load ratio**
  9 axial load ratios σ_0/f_k are considered: $3\ \%, 5\ \%, 8\ \%, 11\ \%, 13\ \%, 16\ \%, 19\ \%, 21\ \%, 24\ \%$
- **Moment distribution factor**
  The moment distribution factor ψ describes the moment profile within the wall and represents the interaction of the wall with the slabs. A factor of $\psi = 0.5$ corresponds to fixed-fixed condition and $\psi = 1.0$ to a cantilever.

The parametric study expands and condenses the existing test experimental grid used for validation. The objective is to investigate the transition areas between the specific failure modes in more detail by varying the main influencing parameters. Of particular importance is the moment distribution in the wall, which strongly influences the simulation results and can vary considerably in real buildings and has not been sufficiently investigated so far.

2.5. Results of the parametric study

This section presents selected results of the parametric study for the brick UNIPOR WS10 CORISO calculated with the presented simulation model. The focus of the evaluation is the determination of the load-bearing and deformation capacities as well as the identification of the occurring failure modes. The decisive failure modes are subdivided into Flexural failure (FL), diagonal tensile failure of the brick (TE) and friction failure (FR). For illustrative purposes, the previously mentioned failure modes are color coded as shown in Figure 6. Since a clear assignment to the failure modes is not always possible, so-called mixed failure modes are also taken into account. Mixed failure modes are combinations of the basic failure modes and represented by the colored overlapping areas shown in Figure 6.

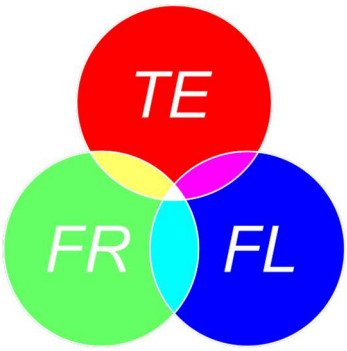

Figure 6: Basic failure modes and their combinations (Boesen 2021)

Figure 7 shows the identified failure modes as a function of the vertical load level σ_0/f_k, the wall slenderness *h/l*, and the moment distribution the moment distribution factor ψ. The individual areas shown represent constant moment distribution factors of 0.5, 0.75, 1.0, and 1.5 and have been shown spatially only for a better understanding. With the three-dimensional representation, a basic differentiation and demarcation of the failure modes with respect to the influencing factors is already recognizable through the color coding.

The graphical representation of failure mechanism as a function of the varied parameters shows a distinct demarcation between flexural and shear failure for the moment distribution factors considered, represented by an oblique boundary lines on each area with constant moment distribution factor. Regardless of the moment distribution, shear failure occurs primarily when the wall slenderness is low and/or the vertical load level is high. Depending on the specific parameter combination, the range of shear failure can be further

divided into friction failure, which occurs at low vertical load level and low wall slenderness, and diagonal tensile failure, which prevails at high vertical load level and low wall slenderness. Furthermore, the representation show, that the moment distribution has a significant influence on the failure mechanism. With higher moment distributions factors, flexural failure becomes increasingly dominant, while with decreasing moment distribution factors, shear failure increasingly occurs. Considering the upper and lower limits of the moment distribution factor, for ψ = 1.5 essentially flexural failure occurs and for ψ = 0.5 essentially shear failure occurs. Based on the results, a simplified criterion can be derived to distinguish the flexural and shear failure considering the vertical load level, the wall slenderness, and the moment distribution within the wall. The criterion can be defined with the shear slenderness λ_{v0} extended with the inverse utilization level f_k/σ_0:

$$\lambda_{v0} = \psi \cdot \frac{h}{l} \cdot \frac{f_k}{\sigma_0} \tag{1}$$

The evaluation of the simulation results leads to a limit value of $\lambda_{v0} = 12$ to differentiate between the failure modes. For smaller values a shear failure occurs, while larger values result in flexure failure. This criterion allows a better prediction of the failure modes comparted to current standards, which very often predict diagonal tension failure, although test results clearly show flexural failure modes (Boesen 2021).

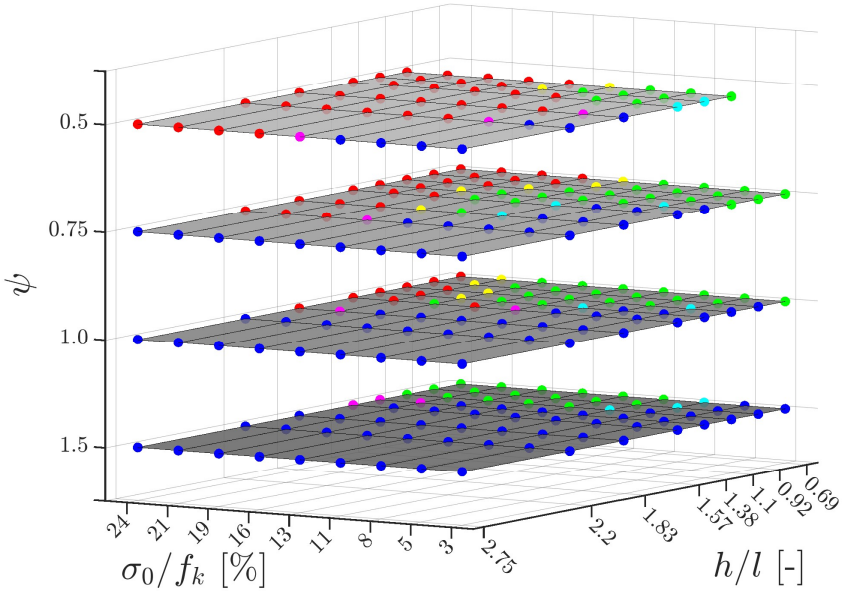

Figure 7: Failure modes in dependence of load level, wall slenderness and moment distribution factor (Salentin 2022)

Figure 8 shows the maximum shear capacity for wall lengths of 1.0 m, 1.5 m, 2.0 m, 3.0 m, and 4.0 m as a function of the vertical load level for four different moment distribution factors. The shapes of the curves basically correspond to the shape of the failure curve according to Mann and Müller (1978). The functional ranges of the curves with flexural or friction failure show a linear course, whereas the ranges with diagonal tensile failure becomes nonlinear with larger slopes. The load-displacement curve confirm that slender walls tend to flexural failure, whereas squat walls tend to fail in shear. As the moment distribution factor increases, the failure of the walls changes more and more to a flexural failure. The change for slender walls of 1.0 m and 1.5 m already occurs at moment distribution factors of ψ = 0.50 - 0.75, whereas the change for walls of 2 m with ψ = 1.0 - 1.5 occurs somewhat later. In contrast, longer walls continue to fail in shear even for higher moment distribution factors.

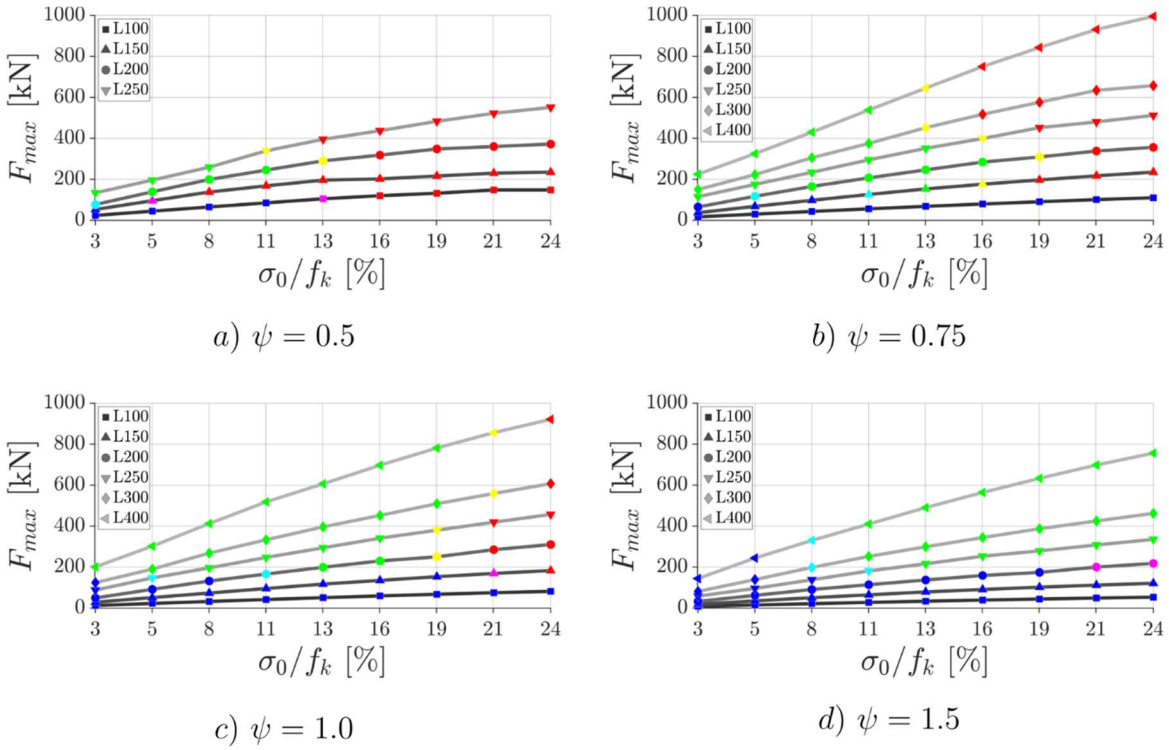

Figure 8: Maximum shear capacities with respect to vertical load level, wall length and moment distribution factor (Salentin 2022)

3. Summary

This paper presents a new database for vertically perforated clay brick masonry used in Germany. Cyclic shear wall test results of the database are evaluated in terms of failure modes, load-bearing and deformation capacities and used as a basis for systematic nonlinear numerical simulations. The numerical model is calibrated by means of small specimen tests and validated with results of shear wall tests. Utilizing the calibrated and validated numerical simulation model an extensive parametric study with variation of all relevant influencing parameters affecting the load-bearing and deformation behavior of the shear walls is carried out. Based on the results, a simplified criterion is derived to differentiate between flexural and shear failure considering the vertical load level, the wall slenderness, and the moment distribution within the wall.

4. Acknowledgement

The authors gratefully acknowledge the collaboration with the Arbeitsgemeinschaft Mauerziegel im Bundesverband der Deutschen Ziegelindustrie e.V. within the IGF Project No. 20988 N/2 “New approaches for the realistic design of masonry structures under horizontal loads” financially supported by the German Federation of Industrial Research Associations (AIF).

5. References

Boesen N. (2021). Trag- und Verformungsverhalten von unbewehrten Mauerwerksscheiben unter Berücksichtigung der Interaktion mit der Gebäudestruktur, Dissertation, RWTH Aachen University – Chair of Structural Analysis and Dynamics

Butenweg C., Lins R., El-Deib K. (2023). Durchführung von Schubwandversuchen an Ziegelmauerwerk – Bericht 1001-2023, *Versuchsbericht*, RWTH Aachen University - Center for Wind and Earthquake Engineering

D'Altri A. M., Sarhosis V., Milani G., Rots J., Cattari S., Lagomarsino S. (2019): Modelling Strategies for the Computational Analysis of Unreinforced Masonry Structures: Review and Classification. In: *Archives of Computational Methods in Engineering*, S. 1–33.

Deutsches Institut für Bautechnik: Allgemeine bauaufsichtliche Zulassung – Z-17.1- 1021. Mauerwerk aus Planhochlochziegeln UNIPOR WS10 CORISO im Dünnbettverafhren mit gedeckelter Lagerfuge, Berlin, 2016.

DIN EN 1052-3: Prüfverfahren für Mauerwerk – Teil 3: Bestimmung der Anfangsscherfestigkeit (Haftscherfestigkeit), 2007

ESECMaSE (2007). D7.1a Test results on the behaviour of masonry under static (monotonic and cyclic) in plane lateral loads, *Collective research report*, University of Kassel – Institute of Structural Engineering

ESECMaSE (2008a). D7.1b Test results on the behaviour of masonry under static cyclic in plane lateral loads, *Collective research report*, Technical University Munich – Department of civil engineering and geodesy

ESECMaSE (2008b). D7.1c Test results on the behaviour of masonry under static cyclic in plane lateral loads, *Collective research report*, University of Pavia – Department of Structural Mechanics

Fehling E., Stürz J. (2009). Horizontalkraft-Tragfähigkeit von Außenwandkonstruktionen aus Wärmedämmziegeln, *Forschungsbericht*, Universität Kassel – Fachgebiet Massivbau

Fehling E., Pfetzing T. (2018). Schubtragfähigkeit von teilweise aufstehenden Mauerwerksscheiben aus Ziegeln, *Forschungsbericht*, Universität Kassel – Fachgebiet Massivbau

Frumento S., Magenes G., Morandi P., Calvi G. M. (2009): Interpretation of experimental shear tests on clay brick masonry walls and evaluation of q-factors for seismic design, *IUSS-Press*

Lemmen P. P. M., Meijer G. J., Rasmussen E. A (1999): Dynamic behavior of composite ship structures (DYCOSS) failure prediction tool, *70th shock and vibration symposium*

Lourenco P. B. (1996): Computational strategies for masonry structures, *Delft University of Technology*

LS-DYNA (2020): Livermore Software Technology Corp. (LSTC). Livermore.

Malvar, L. J., Crawford J. E., Wesevich J. W., Simons D (1997): A plasticity concrete material model for DYNA3D, *International Journal of Impact Engineering 19*, S. 847–873

Mann W., Müller H. (1978): Schubtragfähigkeit von Mauerwerk, *Mauerwerk-Kalender 3*, S. 35–65

Mistler M. (2006): Verformungsbasiertes seismisches Bemessungskonzept für Mauerwerksbauten. *Dissertation*, RWTH Aachen University

Salentin N. (2022). Neues Nachweiskonzept für Mauerwerksbauten aus Ziegelmauerwerk mit Berücksichtigung der Wand-Deckeninteraktion, *Masterthesis*, RWTH Aachen University – Chair of Structural Analysis and Dynamics

prCEN/TS 1998-1-101 Eurocode 8 – Design of structures for earthquake resistance Part 1-101, Characterisation and qualification of structural components for seismic applications by means of cyclic tests.

Schermer D. (2008): Vorschlag für ein neues Schubprüfverfahren, *Mauerwerk-Kalender 33*, S. 705–709.

Schermer, D., Schmalz J., Meyer U. J., Gams M., Lutman M., Triller P. (2018): Shear tests on thermal insulating clay unit masonry walls with thin layer mortar: Schubtragfähigkeit von wärmedämmendem Ziegelmauerwerk, *Mauerwerk 22*, S. 385–398

Schipperen, J. H. A. (2012): Validation of a progressive failure prediction tool for a dynamically loaded three-dimensional composite ship structure, *ECCM15-15th European Conference on Composite Materials*, Venice, Italy, 24-28 June 2012, 1-8

Schlegel R. (2004): Numerische Berechnung von Mauerwerkstrukturen in homogenen und diskreten Modellierungsstrategien

Wu Y.; Crawford J. E. (2015): Numerical modeling of concrete using a partially associative plasticity model, *Journal of Engineering Mechanics 141*, S. 4015051

ZAG (2017). Report P 455/17-610-1 – Seismic response of masonry walls by experimental testing, *Test results*, Department for Structures – Section for Building Structures and Earthquake Engineering, Ljubljana

ZAG (2018b). Report P 455/17-610-2 – Seismic response of masonry walls by experimental testing, *Test results*, Department for Structures – Section for Building Structures and Earthquake Engineering, Ljubljana

ZAG (2018c). Report P 577/18-610-1 – Seismic response of masonry walls by experimental testing, *Test results*, Department for Structures – Section for Building Structures and Earthquake Engineering, Ljubljana

ZAG (2019). Report No. 160/19-610-1 – Seismic response of masonry walls by experimental testing, *Test results*, Department for Structures – Section for Building Structures and Earthquake Engineering, Ljubljana

ZAG (2020a). Experimental Testing of masonry walls – Cyclic shear tests, *Test results*, AGMZ, Department for Structures – Section for Building Structures and Earthquake Engineering, Ljubljana

ZAG (2020d). Experimental Testing of masonry walls – Cyclic shear tests, *Test results*, Department for Structures – Section for Building Structures and Earthquake Engineering, Ljubljana